TRPM7 channels in hippocampal neurons detect levels of extracellular divalent cations

Wen-Li Wei*, Hong-Shuo Sun*[†‡], Michelle E. Olah*, Xiujun Sun[†], Elzbieta Czerwinska*, Waldemar Czerwinski*, Yasuo Mori[§], Beverley A. Orser*[¶], Zhi-Gang Xiong[‖], Michael F. Jackson*[,**], Michael Tymianski[†‡**], and John F. MacDonald*[,**††]

Departments of *Physiology, [††]Pharmacology, [¶]Anesthesia, and [‡]Surgery, University of Toronto, 1 King's College Circle, Toronto, ON, Canada M5S 1A8; [§]Laboratory of Molecular Biology, Department of Synthetic Chemistry and Biological Chemistry, Graduate School of Engineering, Kyoto University, Kyoto 615-8510, Japan; [‖]Robert S. Dow Neurobiology Laboratories, Legacy Research, 1225 Northeast Second Avenue, Portland, OR 97232; and [†]Toronto Western Hospital Research Institute, 11-416 MC-PAV, 399 Bathurst Street, Toronto, ON, Canada M5T 2S8

Edited by Charles F. Stevens, The Salk Institute for Biological Studies, La Jolla, CA, and approved August 20, 2007 (received for review February 7, 2007)

Exposure to low Ca^{2+} and/or Mg^{2+} is tolerated by cardiac myocytes, astrocytes, and neurons, but restoration to normal divalent cation levels paradoxically causes Ca^{2+} overload and cell death. This phenomenon has been called the "Ca^{2+} paradox" of ischemia–reperfusion. The mechanism by which a decrease in extracellular Ca^{2+} and Mg^{2+} is "detected" and triggers subsequent cell death is unknown. Transient periods of brain ischemia are characterized by substantial decreases in extracellular Ca^{2+} and Mg^{2+} that mimic the initial condition of the Ca^{2+} paradox. In CA1 hippocampal neurons, lowering extracellular divalents stimulates a nonselective cation current. We show that this current resembles TRPM7 currents in several ways. Both (*i*) respond to transient decreases in extracellular divalents with inward currents and cell excitation, (*ii*) demonstrate outward rectification that depends on the presence of extracellular divalents, (*iii*) are inhibited by physiological concentrations of intracellular Mg^{2+}, (*iv*) are enhanced by intracellular phosphatidylinositol 4,5-bisphosphate (PIP_2), and (*v*) can be inhibited by Gαq-linked G protein-coupled receptors linked to phospholipase C β1-induced hydrolysis of PIP_2. Furthermore, suppression of TRPM7 expression in hippocampal neurons strongly depressed the inward currents evoked by lowering extracellular divalents. Finally, we show that activation of TRPM7 channels by lowering divalents significantly contributes to cell death. Together, the results demonstrate that TRPM7 contributes to the mechanism by which hippocampal neurons "detect" reductions in extracellular divalents and provide a means by which TRPM7 contributes to neuronal death during transient brain ischemia.

calcium paradox | divalent cation sensing | siRNA | ischemia

Intracellular divalent cations regulate multiple cellular functions; however, the role of extracellular divalent cations in cellular signaling processes remains poorly defined. In isolated myocardium, perfusion with Ca^{2+}-free solution is associated with an influx of Na^+. Paradoxically, the restoration of extracellular Ca^{2+} caused an increase in intracellular Ca^{2+} above baseline and delayed cell death (1). This "Ca^{2+} paradox" likely contributes to the reperfusion injury that follows myocardial ischemia (1). Similar phenomena are observed in other tissues, but, in some cases, both extracellular Ca^{2+} and Mg^{2+} must decrease for the induction of injury (1). An analogous Ca^{2+} paradox has been proposed to underlie ischemia–reperfusion injury in the brain (2), where large decreases in extracellular Ca^{2+} are associated with brain ischemia. These occur as a result of the excitotoxic release of glutamate and consequent membrane depolarization, which act in concert to activate two major influx pathways for Ca^{2+}, namely NMDA receptors and voltage-dependent Ca^{2+} channels (3–5). A large reduction in the extracellular concentration of Mg^{2+} (6) was recently shown to occur in the ischemic brain, confirming that both extracellular Ca^{2+} and Mg^{2+} are simultaneously reduced. The precise mechanism by which neurons respond to changes in the extracellular concentration of divalent cations remains unclear.

In cultured and isolated hippocampal neurons, we previously showed that an inward cation current is transiently activated when the concentration of extracellular divalents is reduced (7, 8). A similar response was observed in CA1 pyramidal neurons in brain slices (9). This current was correlated with a graded disinhibition of a 36-pS nonselective cation channel (7). We previously referred to this channel as the calcium-sensing nonselective cation channel (I_{csNSC}), the molecular identity of which remains elusive.

In seeking a candidate channel for I_{csNSC}, we noted that one member of the melastatin family of transient receptor potential channels, TRPM7, possesses several common properties. These include similar sensitivity to extracellularly applied divalents, similar linear current–voltage relationships in the absence of extracellular divalents and similar single-channel conductance (10, 11). We previously demonstrated the expression of TRPM7 channels in neurons and identified them as key mediators of neuronal death induced by prolonged oxygen/glucose deprivation (OGD) (12). Here, we show, in the absence of OGD, that TRPM7 is an important contributor to the response of neurons to low extracellular divalents suggesting that TRPM7 underlies the previously described I_{csNSC}. Moreover, we show that disinhibition of TRPM7 contributes to cell death in the presence of reduced extracellular divalents. A similar mechanism might contribute to neuronal death during ischemia–reperfusion injury.

Results

We used the "loose-patch" recording technique to demonstrate that changes in the excitability of cultured hippocampal neurons occur with graded decreases in the extracellular concentration of divalents. This technique ensures that excitation does not depend on alterations in the seal resistance of the patch pipette (13, 14) and that there is no disruption in cytosolic constituents. Table 1 lists the composition of the various extracellular solutions used. Cells were initially maintained in a solution containing 1.3 mM Ca^{2+} and 0.9 mM Mg^{2+} (Fig. 1*A*). A transient reduction (30 s) of extracellular

Author contributions: W.-L.W., H.-S.S., W.C., B.A.O., Z.-G.X., M.F.J., M.T., and J.F.M. designed research; W.-L.W., H.-S.S., M.E.O., X.S., E.C., W.C., Z.-G.X., M.F.J., and J.F.M. performed research; E.C., Y.M., and M.T. contributed new reagents/analytic tools; W.-L.W., H.-S.S., M.E.O., X.S., W.C., B.A.O., Z.-G.X., M.F.J., and J.F.M. analyzed data; and B.A.O., M.F.J., M.T., and J.F.M. wrote the paper.

The authors declare no conflict of interest.

This article is a PNAS Direct Submission.

Abbreviations: OGD, oxygen/glucose deprivation; PIP_2, phosphatidylinositol 4,5-bisphosphate; PLC, phospholipase C; mGluR, metabotropic glutamate receptor; CHPG, (*RS*)-2-chloro-5-hydroxyphenylglycine; MPEP, 2-methyl-6-(phenylethynyl)pyridine; shRNA, short hairpin RNA.

**To whom correspondence may be addressed at: Department of Physiology, Medical Sciences Building, 1 King's College Circle, University of Toronto, Toronto, ON, Canada M5S 1A8. E-mail: mike.jackson@utoronto.ca, mike.tymianski@uhn.on.ca, or j.macdonald@utoronto.ca.

This article contains supporting information online at www.pnas.org/cgi/content/full/0701149104/DC1.

Table 1. Extracellular solutions

Solution	NaCl, mM	$CaCl_2$, mM	$MgCl_2$, mM	KCl, mM	Hepes, mM
Standard	140.0	1.3	0.9	5.0	25.0
Low Ca^{2+}	140.0	0.2	0.9	5.0	25.0
Ca^{2+}-free	140.0	≈0.02	0.9	5.0	25.0
Low divalent	140.0	0.2	0.2	5.0	25.0
Divalent-free	140.0	≈0.02	≈0.02	5.0	25.0
Low Ca^{2+}, no Mg^{2+}	140.0	0.1	≈0.02	5.0	25.0

pH 7.4 and osmolarity between 315 and 325 mOsm with glucose and 0.0005 tetrodotoxin for neurons.

Ca^{2+} from 1.3 to 0.2 mM ("low Ca^{2+}") enhanced the firing of neurons (Fig. 1*B*) ($n = 7$). This excitation was further enhanced when solutions lacking added Ca^{2+} ("Ca^{2+}-free") were applied (Fig. 1*C*) or when both Ca^{2+} and Mg^{2+} were simultaneously lowered to 0.2 mM ("low divalent") (Fig. 1*D*). An initial voltage-dependent inactivation of action potentials was observed under this latter condition. These changes in frequency are summarized for a series of cells (Fig. 1*E*).

We next examined the response of cultured hippocampal neurons ($n = 8$) to changes in the extracellular divalents. Whole-cell voltage-clamp recordings were done in the presence of tetrodotoxin to suppress action potentials and spontaneous synaptic transmission. Slowly developing inward currents were generated in response to transient (3-s) applications of low-Ca^{2+} (Fig. 1*Fa*) (-46 ± 7 pA, $n = 7$), low-divalent (Fig. 1*Fb*) (-82 ± 15 pA, $n = 7$) or "divalent-free" solution (Fig. 1*Fc*) (-441 ± 52 pA, $n = 7$). The divalent-free solution contained no chelators and had free concentrations of divalents of ≈0.02 mM (15).

We also examined responses in acutely isolated CA1 neurons to changes in extracellular divalents. This preparation offers the advantage of a faster solution exchange and better control over membrane voltage because the branching dendrites of these neurons are sheared off during their preparation. Similar currents were generated in isolated neurons in response to transient (3-s) applications of low-Ca^{2+} (-122 ± 14 pA), low-divalent (-187 ± 22 pA), or divalent-free solution (-392 ± 46 pA) (Fig. 1*G a–c*, respectively; $n = 10$ for each). The rate of current activation was faster in isolated than in cultured neurons in part because of the enhanced rate of solution exchange. We also observed that the current kinetics were substantially faster in cultured neurons when the intracellular solution contained CsF (standard for isolated cells) rather than Cs-gluconate (standard for cultured cells).

Next, we examined whether HEK293 cells expressing TRPM7 channels also responded to changes in the extracellular concentration of divalents. Recombinant TRPM7 channels generated a large inward current ($-2{,}264 \pm 165$ pA, $n = 10$) when divalent-free solutions were applied. In addition, graded inward currents were recorded when low-Ca^{2+} (-28 ± 3 pA), low-divalent (-58 ± 4 pA), or low-Ca^{2+}, no added Mg^{2+} (-207 ± 25 pA) solutions were applied to these cells ($n = 10$) (data not shown).

To determine whether the *I–V* characteristics of the current generated by reduced divalents in neurons were consistent with those of TRPM7 currents, voltage ramps (±100 mV) were recorded before and after the application of a divalent-free solution (Fig. 2*A*). To prevent the activation of voltage-dependent Ca^{2+} currents, nifedipine was applied to cultured neurons. In isolated neurons, voltage-dependent Ca^{2+} currents rapidly decrease after breakthrough. We therefore waited for this "run down" to occur before applying voltage ramps. Applications of divalent-free solutions preferentially enhanced inward currents over outward currents, thereby reducing outward rectification (Fig. 2 *B* and *C*) ($n = 6$ for isolated and $n = 10$ for cultured neurons). We quantified this change in isolated neurons. At −100 mV, the inward current was

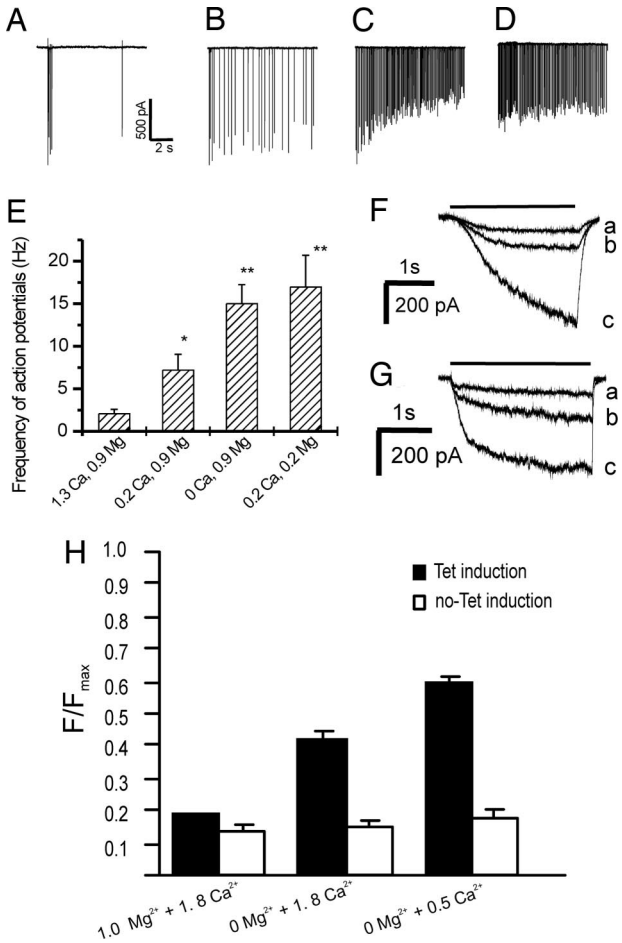

Fig. 1. Cultured hippocampal neurons demonstrate graded responses to reductions in extracellular divalents. (*A–D*) Graded increases in action potential firing frequency are detected when sequentially applying solutions containing 1.3 mM Ca^{2+} and 0.9 mM Mg^{2+} (standard solution) (*A*), 0.2 mM Ca^{2+} and 0.9 mM Mg^{2+} (low Ca^{2+}) (*B*), 0 mM Ca^{2+} and 0.9 mM Mg^{2+} (Ca^{2+}-free) (*C*), or 0.2 mM Ca^{2+} and 0.2 mM Mg^{2+} (low divalent) (*D*). (*E*) For each of these conditions, the change in action potential firing frequency is plotted for a series of six cells and shows the graded excitation. *, $P < 0.05$; **, $P < 0.01$. (*F* and *G*) Whole-cell patch-clamp recordings of currents generated at −60 mV in a cultured (*F*) and isolated (*G*) neuron in response to a change to low Ca^{2+} (*a*), low divalent (*b*), low Ca^{2+}, no Mg^{2+} (*c*). (*H*) In HEK293 cells expressing TRPM7 (Tet induction), a graded increase in cell death is observed when extracellular divalents are progressively reduced. No similar increase is detected in HEK293 cells that do not express TRPM7 (no-Tet induction). Increased cell death is indicated by an increase in the fluorescent ratio F/F_{max}, which represents the estimated fraction of total HEK293 cells that took up propidium iodide.

increased 8.9-fold (from -119 ± 21 to $-1{,}062 \pm 169$ pA) on application of divalent-free solutions. In contrast, at +100 mV, the corresponding outward current was only increased 1.8-fold (from 854 ± 82 to $1{,}578 \pm 206$ pA). Consequently, the rectification ratio (current amplitude at +100 mV divided by the amplitude at −100 mV) was reduced from 9.1 ± 0.1 to 1.9 ± 0.1. A similar change was observed in TRPM7-expressing HEK293 cells (Fig. 1*D*) (12), where the rectification ratio was reduced from 3.2 ± 0.4 ($n = 5$) to 1.9 ± 0.1 ($n = 6$) on application of the divalent-free solution.

We next determined whether lowering extracellular divalents caused a TRPM7-dependent death of HEK293 cells. This expression system allows us to examine TRPM7-dependent cell death in the absence of NMDA receptors, voltage-dependent Ca^{2+} channels, and other factors that contribute to neuronal injury. Control and TRPM7 expressing cells were exposed to three different

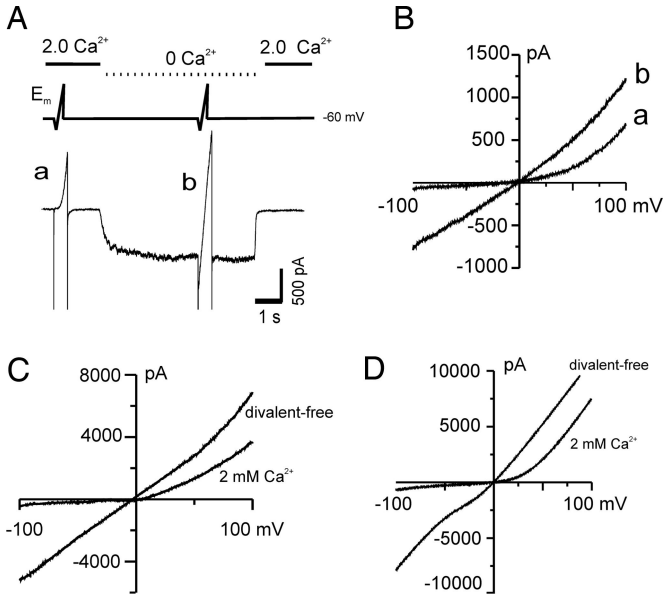

Fig. 2. Divalent-free solutions enhance currents in isolated and cultured neurons as well as TRPM7 currents in HEK293 cells expressing this protein. (*A*) A voltage ramp (±100 mV) was applied for 500 ms from a holding potential of −60 mV to an isolated neuron. The extracellular solution was switched from one containing 2 mM extracellular Ca^{2+} (no Mg^{2+}) (*a*) to a divalent-free solution (*b*). (*B*) On switching to the divalent-free solution, large inward currents were induced and outward rectification was diminished (*b*) in an isolated neuron. (*C* and *D*) A similar response is seen in a cultured hippocampal neuron (*C*) and in a HEK293 cell expressing homomeric recombinant TRPM7 channels (*D*) (also previously shown in ref. 12).

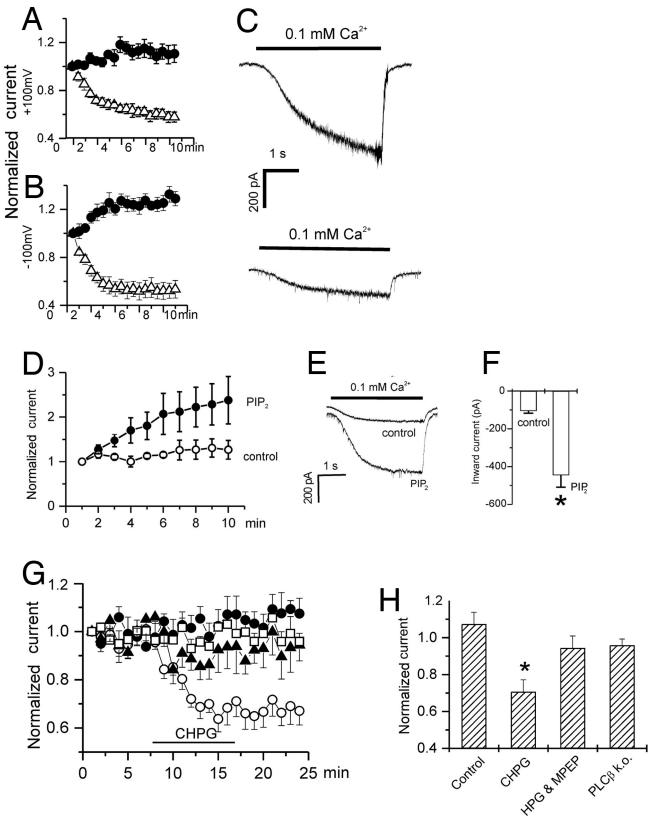

Fig. 3. The time-dependent regulation of responses to lowered divalent cation by intracellular $Mg^{2+}$and PIP_2. Voltage ramps (±100 mV) were used to assess the current amplitudes of isolated neurons in the presence of 1.3 mM extracellular Ca^{2+} (no Mg^{2+}). (*A* and *B*) The amplitude of inward and outward currents increased ($n = 6$) over a period of 5 min using a low concentration of Mg^{2+} (0 $MgCl_2$, 5 mM ATP) in the patch electrode. (*B*) In contrast, when using a relatively high concentration of Mg^{2+} (6 $MgCl_2$, 2 mM ATP), these currents progressively decreased over the first 5 min (△; $n = 8$). (*C*) Responses to applications of low-Ca^{2+} solution to cultured neurons also decreased over this time period (−60 mV) when the high intracellular Mg^{2+} was used. The upper trace shows an example recording of the response after breakthrough, and the lower trace illustrates the response to the same application after 5 min of recording. (*D*) Including PIP_2 (20 μM, $n = 6$) in the patch pipette leads to a time-dependent increase in the inward leak current relative to control recordings without PIP_2 ($n = 6$). (*E*) Responses of isolated neurons to a low-calcium, no Mg^{2+} solution were greater after 10 min of recording with PIP_2 in the patch pipette. There was an increase in inward leak current. (*F*) This current was −105 ± 12 pA in control ($n = 6$) versus −445 ± 64 pA in PIP_2-treated neurons ($n = 8$) (*, difference, $P > 0.01$, Student's *t* test). (*G*) In isolated neurons from WT mice, CHPG inhibited responses to low Ca^{2+}, no Mg^{2+} (applied where indicated by the bar; ○; $n = 10$). This inhibition was blocked by the mGluR5 receptor antagonist MPEP (▲; $n = 6$). A control series of recordings is also shown (no CHPG applied; ●; $n = 7$). The CHPG-induced inhibition was also absent in isolated neurons from PLCβ1 knockout mice (□; $n = 5$). (*H*) Summary graph illustrating inhibition of responses by CHPG (±SEM; *, difference, $P <$ 0.01, Student's *t* test), blockade by MPEP, and lack of inhibition in PLCβ1 knockout mice.

solutions: (*i*) 1 mM Mg^{2+} plus 1.8 mM Ca^{2+}, (*ii*) 0 Mg^{2+} plus 1.8 mM Ca^{2+}, or (*iii*) 0 Mg^{2+} plus 0.5 mM Ca^{2+}. In the absence of TRPM7, cell death was similar in all solutions tested (Fig. 1*H*). In standard concentrations of extracellular divalent cations (1 mM Mg^{2+} plus 1.8 mM Ca^{2+}), TRPM7 expression did not increase cell death. However, removing Mg^{2+} from the extracellular solution more than doubled cell death and a 3-fold increase was observed when Ca^{2+} was also reduced to 0.5 mM (Fig. 1*H*).

In the absence of specific TRPM7 blockers, we determined whether TRPM7-like currents responded in a similar manner to a series of manipulations known to alter TRPM7-mediated currents. We first showed that 2-aminoethoxydiphenyl borate, a blocker of TRPM7 channels, inhibited responses of neurons and TRPM7-expressing HEK293 cells to lowered concentrations of divalent cations [supporting information (SI) Fig. 6].

Endogenous TRPM7 currents are inhibited by physiological concentrations of free intracellular Mg^{2+} (≈0.6 mM) (16–19) but are not regulated by ATP (19). Thus, we tested whether TRPM7-like currents in neurons were modulated by patch solutions designed to either elevate or lower the concentration of Mg^{2+}. The "low" solution ($MgCl_2$ 0, ATP 5 mM) contains virtually no free Mg^{2+}, whereas the "high" solution ($MgCl_2$ 5, ATP 2 mM) has a free concentration close to 2 mM. Changes in the amplitude of outward and inward currents (recorded at +100 and −100 mV, respectively) over time were examined in isolated neurons after breakthrough. In addition, to ensure that the final intracellular Mg^{2+} concentration was not influenced by the influx of Mg^{2+} through TRPM7 channels, recordings were made by using extracellular solutions containing 1.3 or 2 mM Ca^{2+} with no added Mg^{2+}. The presence of 2 mM extracellular Ca^{2+} suppressed but did not eliminate inward currents generated in response to voltage ramps. With low intracellular Mg^{2+}, a time-dependent increase in both outward and inward currents was seen (Fig. 3 *A* and *B*, filled circles) ($n = 7$) ($P < 0.01$ Student's *t* test). In contrast, high intracellular concentrations of Mg^{2+} caused a time-dependent inhibition of the current (Fig. 3 *A* and *B*, open triangles) (holding potential, −60 mV; $n = 9$) ($P <$ 0.01, Student's *t* test). Responses to divalent-free solutions were similarly and progressively inhibited by a high concentration of intracellular Mg^{2+} (Fig. 3*C*).

In whole-cell recordings, the gating of TRPM7 is enhanced by intracellular phosphatidylinositol 4,5-bisphosphate (PIP_2) generation (20) and inhibited via its depletion by phospholipase C (PLC) β-mediated hydrolysis (21, 22). TRPM7-like currents in cultured cortical neurons are also enhanced by the inclusion of PIP_2 in the

NEUROSCIENCE

patch pipette (12). We therefore examined whether the response of neurons to reductions in extracellular divalents was sensitive to changes in intracellular PIP_2 levels. In cultured hippocampal neurons, the inclusion of PIP_2 in the patch pipette caused a progressive increase in the inward holding current at −60 mV (Fig. 3*D*), reflecting an increase in basal TRPM7-like currents. Importantly, inclusion of PIP_2 also increased the responses generated by transient reductions of Ca^{2+} from 1.3 to 0.1 mM and no added Mg^{2+} (Fig. 3 *E* and *F*). Next, we examined whether activation of a known Gαq-linked G protein-coupled receptor inhibited responses in hippocampal neurons via PLCβ-mediated hydrolysis of endogenous PIP_2. Because we previously showed that signaling through Gαq-linked G protein-coupled receptors, including PLCβ1-dependent signaling by metabotropic glutamate receptor 5 (mGluR5), is preserved in isolated hippocampal neurons (23–25), we studied the effect of (*RS*)-2-chloro-5-hydroxyphenylglycine (CHPG), an mGluR5 agonist, on the response to low Ca^{2+}, no Mg^{2+} in these neurons. CHPG inhibited the current and this inhibition was blocked by the mGluR5 antagonist, 2-methyl-6-(phenylethynyl)pyridine (MPEP) (Fig. 3 *G* and *H*). Furthermore, the CHPG-induced inhibition was absent in neurons from PLCβ1 knockout mice (26), which lacked the phospholipase activity necessary to hydrolyze PIP_2 (Fig. 3 *G* and *H*).

To more conclusively demonstrate the contribution of TRPM7 channels to divalent cation detection by neurons, we infected cultured hippocampal cells with an adenovirus containing a vector encoding a short hairpin RNA (shRNA) that targets TRPM7 transcripts ($shRNA_{TRPM7}$). A scrambled shRNA ($shRNA_{control}$) sequence was infected in sister cultures. Both constructs incorporated a GFP domain to identify infected cells. We first tested the effect of this treatment on the expression of TRPM7 in cultured hippocampal neurons using immunocytochemistry. The presence of TRPM7 could be seen as a diffusely distributed signal (in red) in the processes and cell bodies of pyramidal shaped neurons (Fig. 4*A*). Infection with $shRNA_{TRPM7}$ substantially reduced the TRPM7 fluorescent signal compared with either WT cells or those transfected with $shRNA_{control}$ (Fig. 4*B*). As a control, we examined the immunosignal for the related TRPM2 channel, activation of which leads to large inward currents in cultured hippocampal neurons (data not shown). The expression of TRPM2 was unaltered by transfection of cells with $shRNA_{TRPM7}$ indicating the selectivity of the TRPM7 "knockdown" (Fig. 4*C*). The fluorescence intensity of the TRPM7 and TRPM2 signals was quantified, and the selectivity of shTRPM7 was confirmed (Fig. 4 *D* and *E*). In cultured hippocampal neurons, we also confirmed the presence of transcripts for TRPM7 as well as those of other TRP channels including several members of the TRPM class (e.g., TRPC5, TRPM2, and TRPM6) (SI Fig. 8). Treatment of cultures with $shRNA_{TRPM7}$ selectively reduced transcripts for TRPM7 but not those for closely related TRPM6 or TRPM2 (SI Fig. 8).

Given that $shRNA_{TRPM7}$ selectively depressed the expression of TRPM7, we recorded from neurons treated with $shRNA_{control}$ or $shRNA_{TRPM7}$ and assayed the current generated by a solution containing low Ca^{2+} and no Mg^{2+}. In some of these recordings, the cell contents were aspirated via the patch electrode for determination of TRPM7 message (Fig. 5*A*). Currents in cells infected with $shRNA_{TRPM7}$ were decreased by 50% compared with those infected with $shRNA_{control}$ (Fig. 5*B*) ($shRNA_{control}$, $n = 10$, -167 ± 20 pA; $shRNA_{TRPM7}$, $n = 13$, -343 ± 56 pA; $P < 0.001$). We also determined whether the enhancement by PIP_2 was altered in cultures treated with $shRNA_{TRPM7}$. In $shRNA_{TRPM7}$-treated cells, the enhancement of the response after intracellular application of PIP_2 was also reduced relative to control cultures infected with $shRNA_{control}$ (Fig. 5*C*).

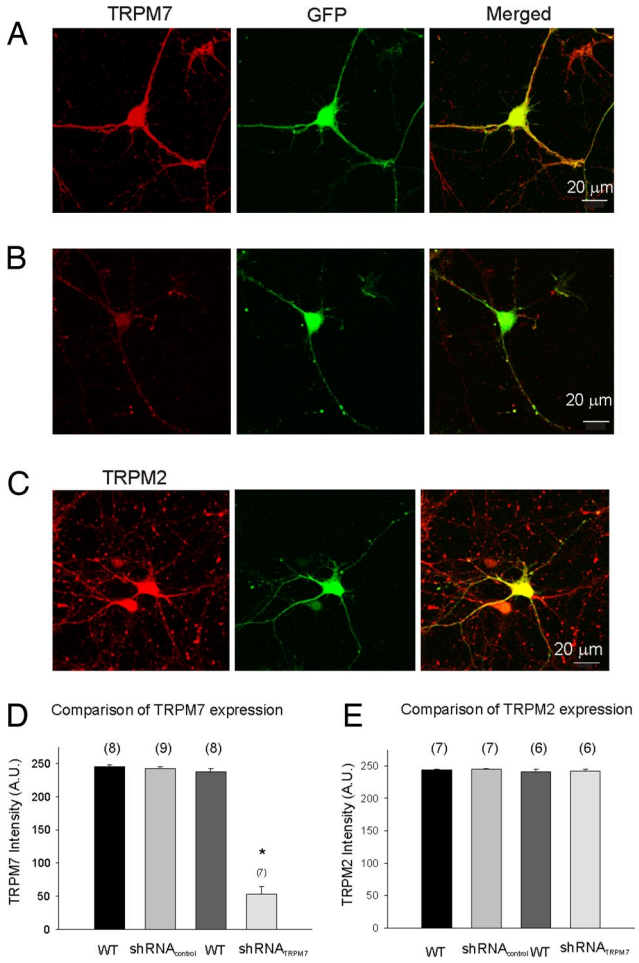

Fig. 4. Immunocytochemistry confirmed the depression of TRPM7, but not TRPM2, protein in neurons treated with adenovirus $shRNA_{TRPM7}$. (*A*) Confocal images at high magnification (×63) show an $shRNA_{control}$/GFP-infected (GFP-expressing; green; *Center*) cultured neuron immunostained for TRPM7 (red; *Left*); merged image is shown (*Right*). (*B*) A similar neuron infected with $shRNA_{TRPM7}$/GFP is shown imaged for the TRPM7 (red; *Left*), GFP (green; *Center*), and merged (*Right*). There was a demonstrable reduction in the level of expression of TRPM7. GFP-positive cells were confirmed as neurons by triple immunostaining the cultures with a neuronal marker, anti-NeuN antibody (blue; not shown). (*C*) No suppression in protein level of TRPM2 was observed in the $shRNA_{TRPM7}$ group. TRPM2 (red; *Left*) colocalized with GFP (green; *Center*) and the merged images (*Right*) indicated a strong overlap of signals. (*D*) A comparison of fluorescence intensities of antibody staining from cell bodies of WT neurons (GFP negative) taken from the same field for each treatment group and neurons infected with $shRNA_{control}$ or $shRNA_{TRPM7}$. Numbers of neurons for each group are as indicated on the top of each bar. A.U., arbitrary unit. *, difference, $P < 0.05$, ANOVA; $P < 0.01$, multiple comparison test (Fisher's least significant difference test). (*E*) TRPM2 fluorescence intensity was unaltered by treatment with $shRNA_{TRPM7}$.

Discussion

We previously showed that prolonged OGD, via production of reactive oxygen/nitrogen species, activates a nonselective cation current (I_{OGD}) that is associated with Ca^{2+} overloading and subsequent neuronal death (12). We then demonstrated that the suppression of TRPM7 expression blocked I_{OGD} and greatly reduced the uptake of Ca^{2+} as well as the neuronal death resulting from OGD. We now show an additional function of TRPM7, namely of providing a means by which neurons detect changes in the extracellular concentration of divalents. Indeed, we suggest that TRPM7 is a major contributor to the previously described neuronal cation current generated in response to reductions in extracellular divalents (I_{csNSC}). Furthermore, in the absence of metabolic stress, we show that lowering extracellular divalents can itself activate TRPM7 channels and thereby contribute to cell death.

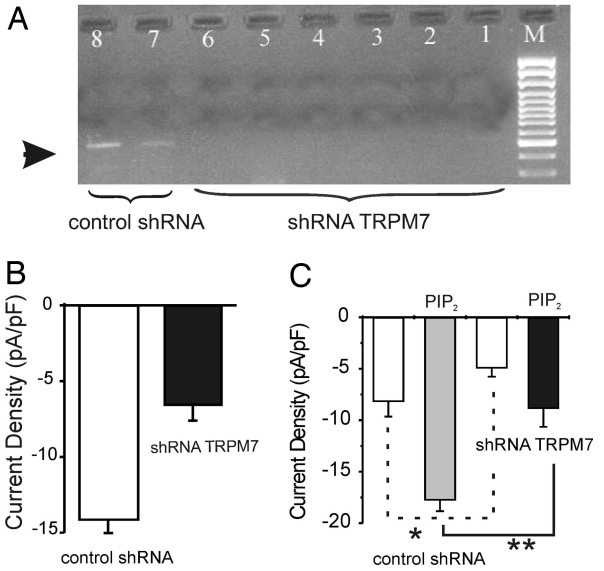

Fig. 5. Infection with $shRNA_{TRPM7}$ reduces the level of TRPM7 message and the responses to low-Ca^{2+}, no Mg^{2+} solutions in cultured neurons. Responses were recorded from 26 neurons and subsequently harvested for single-cell RT-PCR. TRPM7 message was detected in 75% of the $shRNA_{control}$-treated neurons but only 28% of the $shRNA_{TRPM7}$ cells. (*A*) Results from eight representative cells. Control cells from lanes 7 and 8 demonstrate a robust response to divalent-free solution, whereas the six $shRNA_{TRPM7}$ treated cells (lanes 1–6) showed reduced responses to lowering extracellular divalents. (*B*) Group data demonstrating a decrease in current density of these responses in $shRNA_{TRPM7}$-treated neurons versus control ($n = 10$ for $shRNA_{control}$, $n = 13$ for $shRNA_{TRPM7}$). (*C*) Enhancement of responses with PIP_2 in the patch pipette from neurons infected with $shRNA_{TRPM7}$ versus $shRNA_{control}$. Individual cells were not subjected to single-cell PCR for these recordings. In $shRNA_{control}$ neurons, the low Ca^{2+}, no Mg^{2+} current density was increased from -8.2 ± 1.3 pA/pF to -17.8 ± 1.1 pA/pF ($n = 10$) by PIP_2, whereas in $shRNA_{TRPM7}$ neurons, the current density was increased from -4.9 ± 0.8 pA/pF to -8.9 ± 1.8 pA/pF ($n = 12$) (Student's *t* test, $P < 0.01$). *, difference, $P < 0.05$; **, difference, $P < 0.01$.

This and a previous study (7) showed that cultured and acutely isolated neurons are readily depolarized and excited by decreases in the extracellular concentration of Ca^{2+} and/or Mg^{2+}. Neurons respond to such decreases with graded inward currents mediated, at least in part, by a nonselective cation channel of ≈36 pS (7), similar to the conductance of TRPM7 channels (≈40 pS) (20).

TRPM7 currents in various cell lines can be regulated by the intracellular levels of Mg^{2+} (10) and PIP_2 (21, 27). In addition, TRPM7 currents can be blocked by 2-aminoethoxydiphenyl borate. Similarly, responses to divalent-free solution in neurons were inhibited by elevating free intracellular Mg^{2+} and conversely enhanced when intracellular free Mg^{2+} was reduced. The time dependence of these effects was similar to that reported for TRPM7 currents in other cell types (16–19). Also consistent with an involvement of TRPM7, increasing intracellular PIP_2 enhanced the response of neurons to low Ca^{2+} and no Mg^{2+}. Importantly, infection of cultured hippocampal neurons with $shRNA_{TRPM7}$ depressed this effect of PIP_2. Furthermore, in isolated neurons, stimulation of mGluR5 receptors leads to a PLCβ1-dependent inhibition of this response, consistent with hydrolysis of endogenous PIP_2 causing a decrease in TRPM7 activity. Finally, in parallel experiments, the responses of neurons and HEK293 cells expressing TRPM7 to the divalent-free solution could be blocked by 2-aminoethoxydiphenyl borate (SI Fig. 6).

More direct evidence implicating TRPM7 as a mediator of the neuronal response to low divalents was obtained by using a specific shRNA sequence ($shRNA_{TRPM7}$) to suppress the expression of TRPM7. The effectiveness and selectivity of this approach was confirmed by immunostaining (Fig. 4) and RT-PCR (Fig. 5). Treatment with $shRNA_{TRPM7}$ reduced the response to low Ca^{2+}, no Mg^{2+} by ≈50%, indicating that it depends, in large part, on TRPM7. The residual current can be attributed in part to an incomplete suppression of TRPM7 and partial contribution by other divalent cation sensitive conductances (see below).

We also noted some differences between the sensitivity of currents in neurons and those generated by homomeric TRPM7 channels in HEK293 cells to various inhibitors. In cultured neurons, the IC_{50} values for inhibition of the response to divalent-free cation solution are as follows: −60 mV, IC_{50}: Gd^{3+}, 1.4 μM; neomycin, 4.3 μM; Ca^{2+}, 150 μM; Mg^{2+}, 340 μM (7); compared with monovalent TRPM7 recombinant currents in HEK293 cells: −60 mV, IC_{50}: Gd^{3+}, 2.5 μM; Mg^{2+}, 4.3 μM; La^{3+}, 17 μM; Ca^{2+}, 27 μM (SI Fig. 7). Several reasons for these differences are likely the following. (*i*) TRPM7 can form heteromeric channels with TRPM6 (28). Different types of TRPM7 containing channels may therefore exist in neurons. (*ii*) TRPM7-containing channels in neurons may interact with proteins (e.g., adaptor, signaling, and scaffolding proteins) that are absent from HEK293 cells. (*iii*) Finally, other divalent-cation sensitive channels (29, 30) may have partially contributed to the response in neurons. Examples include the following: voltage-dependent Ca^{2+} (31), nucleotide-gated (32), stretch-activated cation (33), gap junction hemichannels (34), and proton-gated channels (35).

On the basis of our findings, and drawing on existing knowledge of mechanisms contributing to the Ca^{2+} paradox, we propose an extended model of how TRPM7 contributes to neuronal cell death during ischemia–reperfusion injury. During the initial stages of an ischemic attack, the resulting reduction in the extracellular divalents causes an increase in monovalent cation permeability and intracellular loading of Na^+ (36, 37). We propose that TRPM7 contributes to this initial Na^+ loading phase and associated toxicity. Indeed, in the absence of divalent cations, TRPM7 channels are primarily permeable to monovalent cations (Na^+ and K^+) (10, 11). The resulting inward TRPM7 currents will largely be carried by monovalent cations, but divalent cations will also enter the cell as long as there is a permissive concentration gradient. Reperfusion provokes a dramatic influx of Ca^{2+}, increased production of reactive oxygen/nitrogen species, and loss of cell viability (36–38). Although the restoration of extracellular divalents during this phase will reduce the contribution of TRPM7, this will be offset by the production of reactive oxygen/nitrogen species, which facilitate TRPM7 currents (12). In this context, it is worth noting that TRPM7 currents need not be large to induce cell death (39).

Through these mechanisms, TRPM7 will add to and exacerbate neuronal injury mediated by other previously described mechanisms. For example, the Na^+ loading of cells may lead to reversal of the sodium–calcium exchanger (1) and subsequent loading of intracellular Ca^{2+} after its extracellular restoration. By contributing to Na^+ loading, TRPM7 may prime the system for its eventual demise. Furthermore, ischemia may, via oxidative stress, activate TRPM2 channels that are also permeable to Ca^{2+} (40, 41). The precise contribution of TRPM7 channels to the various phases of toxicity will require selective TRPM7 blockers. However, the present findings provide important insight into a mechanism by which TRPM7 contributes to neuronal signaling under pathological conditions. Collectively, our studies suggest that TRPM7 represents an important target for the development of future antiexcitotoxic treatments.

Materials and Methods

Cultured mouse hippocampal neurons were grown as described in ref. 7 and used for recordings 14–20 days after plating. For immunocytochemistry, low-density hippocampal cultures were prepared from Swiss mice at days 17–19 of gestation (42). We thank Daesoo Kim and Hee-Sup Shin (Korean Institute of Science and Technology, Seoul, South Korea) for providing the PLCβ1 knock-

out mice. CA1 hippocampal neurons were acutely isolated by using an approach modified after Wang and MacDonald (43). Data were obtained from large pyramidal cells that were phase-bright, clearly outlined, and lacked signs of swelling or damage. HEK293 cells, transfected with Flag-murine TRPM7/pCDNA4-TO (kind gift from A. Scharenberg, Seattle WA), were grown with DMEM supplemented with 10% FBS, blasticidin (5 μg/ml), and zeocin (0.4 mg/ml). TRPM7 expression was induced by adding 1 μg/ml tetracycline to the medium (12). Whole-cell recordings were made 18–48 h after induction by using an Axopatch-1B amplifier (Molecular Devices, Sunnyvale, CA). Input resistance was monitored by applying a voltage step of −10 mV. Only recordings with a pipette-membrane seal >2 GΩ were included. A rapid perfusion system was used to achieve exchange of solutions (τ of exchange, ≈2 ms). Current–voltage relationships were obtained by using a voltage ramp (±100 mV, 500 ms) applied from a holding potential of −60 mV (in neurons) or 0 mV (in HEK293 cells). Unless stated otherwise, the pipette solution for neurons contained the following (in mM): 140 CsF or Cs-gluconate, 35 CsOH, 10 Hepes, 2 tetraethylammonium chloride, 11 EGTA, 1 $CaCl_2$, 2 $MgCl_2$, 2 K_2ATP (pH 7.3, 290–300 mOsm/liter). The free $[Mg^{2+}]_i$ was ≈0.28 mM according to www.stanford.edu/~cpatton/maxc.html. The pipette solution for recordings in HEK293 cells contained the following (in mM): 145 Cs-methanesulfonate, 8 NaCl, 5 ATP, 1 $MgCl_2$, 10 EGTA, 4.1 $CaCl_2$, and 10 Hepes (pH 7.3, 290–300 mOsm/liter) (free $[Mg^{2+}]_i$ was ≈0.1 mM). RT-PCR of single cultures or single cells is described in *SI Methods*.

Mouse cultured hippocampal neurons grown on coverslips and treated with adenovirus $shRNA_{control}$ (scrambled RNAi) or $shRNA_{TRPM7}$ (TRPM7 RNAi) were washed in PBS. These were fixed in 2.5% sucrose with 4% paraformaldehyde in PBS at room temperature for 20 min. Immunostaining was performed as described previously in ref. 44. In brief, neurons were blocked by using 1% BSA, 3% rabbit serum, and 0.3% Triton X-100 in PBS solution for 90 min at room temperature and double or triple labeled with goat anti-TRPM7 Ab (ab729; 1:50; Abcam, Cambridge, MA) or rabbit anti-TRPM2 Ab (ab11168; 1:50; Abcam), and mouse anti-NeuN Ab (1:100; Chemicon, Temecula, CA) overnight at 4°C (gently rocking). Neurons were subsequently washed with PBS, blocked, and incubated with rabbit anti-goat Alexa 568 (1:100; Molecular Probes, Eugene, OR), goat anti-rabbit Alexa 568 (1:100; Molecular Probes), and goat anti-mouse Alexa 350 (1:200; Molecular Probes) for 1 h at room temperature. After washing, coverslips were then mounted by using ProLong Gold antifade reagent (Molecular Probes) and viewed with a confocal laser-scanning microscope (LSM 510 META; Zeiss) using a ×63 lens. Optical stacks of 5–10 confocal images (0.5-μm intervals) were used to generate figures (green, GFP; red, anti-TRPM7 or TRPM2; blue, anti-NeuN). In each field, fluorescent intensity of the anti-TRPM7 or anti-TRPM2 signal was measured from the cell body of infected (GFP-positive) and uninfected (WT, GFP-negative) neurons by using NIH ImageJ and expressed as arbitrary units. One-way ANOVA was used to compare values obtained among all four groups. If significant differences were identified, a multiple-comparison posttest was applied (Fisher's least significant difference test). Data are presented as mean ± SEM.

Cell death assays were conducted as follows: stable transfected Flag-TRPM7 HEK293 cells were cultured on poly(D-lysine) (Sigma–Aldrich)-coated plates in MEM with 10% FBS supplemented with 20 mM GlutaMAX-1, 100 units/ml penicillin G sodium,100 units/ml streptomycin sulfate, 0.25 μg/ml amphotericin B, 5 μg/ml blasticidin, 0.4 mg/ml zeocin (Invitrogen, Carlsbad, CA), and incubated at 37°C with 5% CO_2. Cells were plated 24 h before tetracycline (1 μg/ml; Invitrogen) induction. After 20 h with or without tetracycline induction, cells were washed twice with Hanks' balanced salt solution (HBSS) (121 mM NaCl, 5 mM KCl, 20 mM D-glucose, 10 mM Hepes acid, 10 mM Hepes-Na, 1 mM Na-pyruvate) and incubated in HBSS (with various concentrations of $CaCl_2$ and $MgCl_2$ as indicated in the text) with 10 μg/ml propidium iodide (Molecular Probes) at 37°C for 48 h. Propidium iodide fluorescence (F) was measured by using a Fluoroskan Ascent FL microplate reader and accompanying Ascent software (Thermo Fisher Scientific) at $\lambda_{excitation}$ = 530 nm, $\lambda_{emission}$ = 620 nm. Maximal fluorescence (F_{max}) was obtained by reading from wells to which 0.05% Triton X-100 was added for 20 min.

This work was supported by Canadian Institutes of Health Research Grants MOP15514 (to J.F.M.) and MOP68939 (to M.T.) and by the Canadian Stroke Network (J.F.M., M.T., and M.F.J.).

1. Piper HM (2000) *Cardiovasc Res* 45:123–127.
2. Young W (1986) *Cent Nerv Syst Trauma* 3:235–251.
3. Morris ME, Trippenbach T (1993) *Am J Physiol* 264:R761–R769.
4. Kristian T, Siesjo BK (1998) *Stroke* 29:705–718.
5. Heinemann U, Stabel J, Rausche G (1990) *Prog Brain Res* 83:197–214.
6. Lin MC, Huang YL, Liu HW, Yang DY, Lee CP, Yang LL, Cheng FC (2004) *J Am Coll Nutr* 23:561S–565S.
7. Xiong Z, Lu W, MacDonald JF (1997) *Proc Natl Acad Sci USA* 94:7012–7017.
8. Xiong ZG, Chu XP, MacDonald JF (2001) *J Neurophysiol* 86:2520–2526.
9. Burgo A, Carmignoto G, Pizzo P, Pozzan T, Fasolato C (2003) *J Physiol (Lond)* 549:537–552.
10. Harteneck C (2005) *Naunyn Schmiedebergs Arch Pharmacol* 371:307–314.
11. Kraft R, Harteneck C (2005) *Pflügers Arch* 451:204–211.
12. Aarts M, Iihara K, Wei WL, Xiong ZG, Arundine M, Cerwinski W, MacDonald JF, Tymianski M (2003) *Cell* 115:863–877.
13. Formenti A, De SA (2000) *Neurosci Lett* 279:49–52.
14. Chu XP, Zhu XM, Wei WL, Li GH, Simon RP, MacDonald JF, Xiong ZG (2003) *J Physiol (Lond)* 550:385–399.
15. Hoth M (1995) *Pflügers Arch* 430:315–322.
16. Hermosura MC, Monteilh-Zoller MK, Scharenberg AM, Penner R, Fleig A (2002) *J Physiol (Lond)* 539:445–458.
17. Kozak JA, Kerschbaum HH, Cahalan MD (2002) *J Gen Physiol* 120:221–235.
18. Prakriya M, Lewis RS (2002) *J Gen Physiol* 119:487–507.
19. Kozak JA, Cahalan MD (2003) *Biophys J* 84:922–927.
20. Kerschbaum HH, Kozak JA, Cahalan MD (2003) *Biophys J* 84:2293–2305.
21. Runnels LW, Yue L, Clapham DE (2002) *Nat Cell Biol* 4:329–336.
22. Ramsey IS, Delling M, Clapham DE (2006) *Annu Rev Physiol* 68:619–647.
23. Lu WY, Xiong ZG, Lei S, Orser BA, Dudek E, Browning MD, MacDonald JF (1999) *Nat Neurosci* 2:331–338.
24. Macdonald DS, Weerapura M, Beazely MA, Martin L, Czerwinski W, Roder JC, Orser BA, MacDonald JF (2005) *J Neurosci* 25:11374–11384.
25. Kotecha SA, Jackson MF, Al Mahrouki A, Roder JC, Orser BA, MacDonald JF (2003) *J Biol Chem* 278:27742–27749.
26. Kim D, Jun KS, Lee SB, Kang NG, Min DS, Kim YH, Ryu SH, Suh PG, Shin HS (1997) *Nature* 389:290–293.
27. Langeslag M, Clark K, Moolenaar WH, van Leeuwen FN, Jalink K (2007) *J Biol Chem* 282:232–239.
28. Penner R, Fleig A (2007) *Handb Exp Pharmacol* 313–328.
29. Formenti A, De SA, Arrigoni E, Martina M (2001) *J Physiol (Lond)* 535:33–45.
30. Xiong ZG, MacDonald JF (1999) *Can J Physiol Pharmacol* 77:715–721.
31. Hablitz JJ, Heinemann U, Lux HD (1986) *Biophys J* 50:753–757.
32. Root MJ, MacKinnon R (1993) *Neuron* 11:459–466.
33. Yang XC, Sachs F (1989) *Science* 243:1068–1071.
34. Malchow RP, Qian H, Ripps H (1993) *J Neurosci Res* 35:237–245.
35. Immke DC, McCleskey EW (2003) *Neuron* 37:75–84.
36. Xin WK, Zhao XH, Xu J, Lei G, Kwan CL, Zhu KM, Cho JS, Duff M, Ellen RP, McCulloch CA, *et al.* (2005) *Eur J Neurosci* 21:622–636.
37. Chinopoulos C, Gerencser AA, Doczi J, Fiskum G, Adam-Vizi V (2004) *J Neurochem* 91:471–483.
38. Piper HM, Meuter K, Schafer C (2003) *Ann Thorac Surg* 75:S644–S648.
39. Monteilh-Zoller MK, Hermosura MC, Nadler MJ, Scharenberg AM, Penner R, Fleig A (2003) *J Gen Physiol* 121:49–60.
40. Chinopoulos C, dam-Vizi V (2006) *FEBS J* 273:433–450.
41. MacDonald JF, Xiong ZG, Jackson MF (2006) *Trends Neurosci* 29:75–81.
42. Sattler R, Xiong Z, Lu WY, Hafner M, MacDonald JF, Tymianski M (1999) *Science* 284:1845–1848.
43. Wang LY, MacDonald JF (1995) *J Physiol (Lond)* 486:83–95.
44. Sun HS, Feng ZP, Miki T, Seino S, French RJ (2006) *J Neurophysiol* 95:2590–2601.